26th ABCM International Congress of Mechanical Engineering
November 22-26, 2021. Florianópolis, SC, Brazil

COB-2021-2258
THERMODYNAMIC-BASED, ONE-DIMENSIONAL PIPELINE WAX DEPOSITION MODEL

Fabio Gaspar Santos Junior
Department of Mechanical Engineering, Pontifical Catholic University of Rio de Janeiro, PUC-Rio
R. Marques de S. Vicente 225, Gavea, 22451-900, Rio de Janeiro, RJ, Brazil
fabiogaspar15@gmail.com

Felipe Pereira Fleming
Petrobras Research and Development Center, Rio de Janeiro, 21914-915, Rio de Janeiro, RJ, Brazil
felfleming@gmail.com

Luis Fernando Alzuguir Azevedo
Ivan Fernney Ibanez Aguilar
Angela Ourivio Nieckele
Department of Mechanical Engineering, Pontifical Catholic University of Rio de Janeiro, PUC-Rio
R. Marques de S. Vicente 225, Gavea, 22451-900, Rio de Janeiro, RJ, Brazil
lfaa@puc-rio.br, iibanez@puc-rio.br, nieckele@puc-rio.br

Abstract. *Wax deposition in oil and gas subsea pipelines is one of the main problems associated with flow assurance. As the oil flows from the reservoir to the platform, it loses heat to the cold ocean environment. Solid crystals appear when the mixture temperature is below the Wax Appearance Temperature. The solids can form deposits at the wall, increasing the required pumping power, or even completely obstructing the flow, resulting in significant maintenance and capital losses. Since pipelines are normally very long, one-dimensional models are required to predict wax deposition along the pipe walls. Wax deposition 1D codes available in the literature are based on molecular diffusion as the main deposition mechanism and require several adjustable empirical constants to fit to field data. In the present work, a novel methodology based on a thermodynamic model for the liquid-solid mixture coupled with 1D hydrodynamic calculation and a 2D heat transfer calculation is employed to predict wax deposit formation. From the flow, pressure and temperature distribution and initial species composition, the solid fraction and all the fluid properties are determined with the aid of the thermodynamic model. It is assumed that the wax deposits are formed when the solid fraction is above 2%. Validation with experimental data obtained from a laboratory-scale annular test section was performed, and reasonable agreement was obtained.*

Keywords: *wax deposition, one-dimensional model, flow assurance, thermodynamic model.*

1. INTRODUCTION

Over the years, oil production advanced to offshore fields reaching greater water depths. In these production scenarios the oil comes from the reservoirs at elevated temperatures, flowing through long pipelines under the sea, loosing heat to the cold ocean environment. In case the oil temperature reaches the critical Wax Appearance Temperature (WAT) some hydrocarbon components may form solids that can produce deposits at the pipe walls. Wax deposit formation is relevant problem for the industry potentially leading to the reduction oil flow rate production and, in extreme cases, to the complete blockage of the line. Chemical injection and mechanical wax removal by pigging are methods frequently employed by the industry to mitigate the wax formation process. However, these methods are associated with additional operational costs (Azevedo *et al.*, 1996; Anisuzzaman *et al.*, 2017).

The capability to predict the occurrence of wax deposits formation is relevant information for pipeline designers and operators. The advance knowledge of the wax deposit's time evolution and spatial distribution can guide the decision of designing thermally insulated lines or to design the frequency of pigging operations. Accurate simulation models of wax deposit formation are, therefore, important tools to aid pipeline designers and operators.

The need to predict wax deposit formation has led to a research effort directed to the understanding of the basic mechanisms governing this phenomenon (Singh *et al.*, 1999; Singh *et al.*, 2000; Azevedo and Teixeira, 2003; Mehrotra *et al.*, 2020).

Most models available in the literature consider molecular diffusion as the main mechanism, although the predictions

from these models are always adjusted to laboratory or field data by the tuning of some model parameters or even flow properties, such as the diffusion coefficient (Burger *et al.*, 1981; Azevedo and Teixeira, 2003; Mahir *et al.*, 2018).

The wax deposit formation has also been modeled as a phase change process governed solely by heat transfer (e.g., Ehsani and Mehrotra, 2019). Other works have investigated different wax deposition mechanisms such as Brownian diffusion (Todi and Deo, 2006) or Shear Dispersion (Van Der Geest *et al.*, 2018). Recently, the wax deposit formation has been modeled as an interaction of the fluid shear stress imposed on the deposit interface and the deposit yield stress. In this model the deposit is considered as a gel-like structure with non-Newtonian behavior and displaying and yield stress dependent on the deposit solid content (Palermo and Tournis, 2015; Zheng *et al.*, 2016).

In all models proposed, predictions of the fluid thermodynamic behavior are implemented with different degrees of complexity. The solution thermodynamics can be represented by a simple experimentally-determined equilibrium curve of a binary mixture of solvent and lumped paraffin components, or by a complex multicomponent thermodynamic model. In the latter, the model predicts local solid fraction and mixture composition as a function of local pressure and temperature (Lira-Galeana *et al.*, 1996; Coutinho *et al.*, 2006).

Multicomponent thermodynamic models produce accurate predictions of fluid composition but require significant computer time. For the prediction of wax deposition in pipelines, these thermodynamic models must be coupled with solutions of the velocity, temperature and species concentration fields. The complexity of these coupled system of equations renders the prediction of the wax deposition in long field pipelines not viable for presently available computer hardware.

The present paper presents an ongoing research effort aimed at combining a one-dimensional hydrodynamic model and a simple 2D heat transfer model suitable for long filed pipelines, with accurate thermodynamic calculations. At the present stage of development, the predictions of this hybrid model are compared with available accurate laboratory-scale experiments. The experiments results were obtained for laminar flow in an annular pipe section. The description of the model developed is described in the next section.

2. MATHEMATICAL EQUATIONS

The wax deposition model proposed here is based on the determination of the solid volume fraction S_s from the fluid thermodynamic behavior (Fleming, 2018). It is assumed that the deposit is formed when the solid fraction is above 2%, as suggested by several authors in the literature (Holder and Winkler, 1965; Veiga *et al.*, 2020). The fluid is modeled as a mixture of liquid and solid and the solid volume fraction in the mixture is defined as

$$S_s = \frac{\forall_s}{\forall_t} = \frac{B_s / \rho_s}{B_s / \rho_s + B_l / \rho_l}, \tag{1}$$

where $\forall_s$ is the solid volume and $\forall_t$ the total volume. B_k and ρ_k are the mass fraction and specific mass of phase k, and are determine with the thermodynamic model of Coutinho *et al.* (2006) based on pressure, temperature and mixture composition. The mixture velocity, pressure and temperature are determined from the conservation equations of mass, momentum and energy.

All mixture properties are obtained with

$$\phi_m = S_s \phi_s + (1 - S_s)\phi_l, \tag{2}$$

where ϕ_m is a mixture property and ϕ_s and ϕ_l are the solid and liquid property dissolved in the mixture. ϕ is a property obtained with the thermodynamic model, it can be density ρ, heat capacity c_p, thermal conductivity k, or viscosity μ (where the viscosity of the solid dissolved in the mixture is considered equal to the liquid viscosity).

2.1 Conservation equations

The present model is to be applied in long pipelines, therefore a 1D flow formulation is developed. However, to be able to obtain a solid fraction distribution along the cross section, a 2D formulation is developed for the temperature and average properties in the pipe cross-section are determined as

$$\overline{\phi_m} = \frac{1}{A_t}\int_{A_t} \phi_m dA_t = 0 \quad ; \quad A_t = A - A_d, \tag{3}$$

where A_t is the free flow cross-section, A is the pipe cross section and A_d is the deposit cross-section area.

To determine the flow, it is assumed that the solid and liquid velocity are equal to the mixture velocity and constant mass flow $\dot{m}$ is imposed along the pipeline, equal to the inlet mass flow, $\dot{m} = \rho_{in}\dot{\forall}_{in}$, where $\dot{\forall}$ is the volumetric flow rate, and the subscript *in* refers to the inlet condition. Thus, the cross-section average velocity $\bar{V}$ is obtained from

$$\frac{\partial \dot{m}}{\partial z} = 0 \quad ; \quad \dot{m} = \bar{\rho}_m \bar{V} A_t, \tag{4}$$

where z is the pipeline axial direction. The velocity is described by a fully developed velocity profile as $V = \bar{V}\, g(r)$, where the function $g(r)$ depends on if the flow is laminar ($Re < 2300$) or turbulent ($Re \geq 2300$). Here, Re is Reynolds number

$$Re = \frac{\bar{\rho}_m \bar{V} D_h}{\bar{\mu}_m} \quad ; \quad D_h = \frac{4A_t}{P_w}, \tag{5}$$

where D_h is the pipe hydraulic diameter and P_w is the wetted perimeter.

Pressure (p) variation along the pipeline is determined from linear momentum conservation equation for a fully developed flow, based on the gravity g and wall shear stress τ_w, which is determined employing a friction factor f as

$$-\frac{\partial p}{\partial z} = \frac{\tau_w P_w}{A_t} - \bar{\rho}_m\, g \sin\alpha \quad ; \; \tau_w = \frac{1}{8} f \bar{\rho}_m \bar{V}^2, \tag{6}$$

where α is the pipeline inclination with the horizontal.

Finally, the temperature can be determined from the mixture energy conservation equation, which is obtained by combining the energy equation for the liquid and solid (Fleming, 2018; Branco, 2019). As mentioned, for the temperature determination, a 2D model is considered. The energy equation, neglecting axial diffusion, compression work and viscous dissipation, is

$$\rho_m c_{pm} \left(\frac{\partial T}{\partial t} + V \frac{\partial T}{\partial z}\right) = \frac{1}{r}\frac{\partial}{\partial r}\left(k_m r \frac{\partial T}{\partial r}\right) - \rho_m \lambda \left(\frac{\partial \chi_l}{\partial t} + V \frac{\partial \chi_l}{\partial z}\right), \tag{7}$$

in which $\lambda = h_l - h_s$ is the phase change term described by the solid-liquid melting enthalpy, where h is the enthalpy and χ_l is the liquid molar fraction present in the mixture.

To solve the conservation equations, temperature above the wax appearance temperature (WAT) and volumetric flow rate were defined at the inlet, as well as the mixture composition. Pressure was imposed at the exit. Deposition will occur by prescribing a cold temperature at the pipeline wall, T_{cold}.

2.2 Thermodynamic properties

The species properties ϕ_{ki} of each phase k and phase properties $\phi_k$were determined based on thermodynamic model of *Multiple Solid Solutions* proposed by Coutinho *et al.* (2006), as a function of pressure, temperature and composition of the mixture. Details of thermodynamic model can be found in da Silva *et al.* (2017) and Fleming (2018).

The concentration of each specie i in the liquid and solid phase in the mixture are determined based on a Flash calculation, enforcing equilibrium between solid and liquid fugacity of each mixture specie i. Thus, when there is wax precipitation, the molar property of each component is obtained, the species in each phase, and finally the mixture properties are determined. As presented in Eq. (1), the solid volume fraction is determined from the mass fraction and specific mass of each phase.

The density, thermal conductivity and viscosity are determined from the reduced properties as proposed by Queimada *et al.* (2005) and Fleming (2018).

At the present work, the total molar concentration of the mixture was considered constant. And a table with all properties as a function of pressure, temperature and composition was created. The necessary properties for the numerical integration of the conservation equations were determined through interpolation of the table.

2.3 Numerical Approach

The conservation equations were discretized based on the Finite Volume method, with the velocity stored at the control volumes face.

To discretize the energy equation, central difference was applied for the diffusive flux, and upwind scheme for the convective flux. Once the deposit is formed, the velocity is set to zero inside the deposit. The temporal discretization was obtained with first order Euler implicit formulation.

To solve the temperature, a marching procedure was applied in the axial direction and the TDMA algorithm was solved to determine its radial variation.

So, the model solution is as follows:

1. Given a fluid composition, a table is generated using the thermodynamic model containing a vast pressure and temperature combination,
2. Initialize the properties, and flow variables, based on boundary conditions.
3. Repeat up to the final desired time instant, by moving forward at time $t = t + \Delta t$:
   3.1. define free cross-section area,
   3.2. obtain velocity and pressure field,
   3.3. calculate temperature field.

3. CASE STUDY

To validate the proposed model, available experimental data of Veiga *et al.* (2020) was selected. The experimental apparatus consisted of an annular pipe, where cold temperature T_{cold} was imposed at the inner radius (r_{in}), while the outer radius (r_{ex}) was kept at a high temperature equal to the inlet temperature T_{in}. The teste section length was equal to L. Atmospheric pressure was defined at the outlet. The test parameters are shown in Table 1. The resulting Reynolds number is 650. Since the experimental test was laminar ($Re < 2300$), the following velocity profile for an annular cross section was defined

$$V = \frac{2(1-RR^2)}{(1-RR^4)+(1-RR^2)^2/\ln(RR)}\bar{V}\left[1-\left(\frac{r}{r_{ex}}\right)^2-\frac{(1-RR^2)}{\ln(RR)}\ln\left(\frac{r}{r_{ex}}\right)\right], \tag{8}$$

where $RR = r_{in}/r_{ex}$ is the radius ratio. The corresponding friction factor is

$$fRe = \frac{64\,(1-RR^2)(1-RR)^2}{[(1-RR^4)+(1-RR^2)^2/\ln(RR)]}, \tag{9}$$

The temporal solution followed the laboratory procedure. Initially, the entire domain is at hot temperature and the inner wall is cooled after the first time-step. Aiming to reproduce the experimental data, a cold wall temperature variation with time was imposed. In the first 40 seconds after cooling initiated, the wall temperature dropped from 38 to 17.6 ºC, after more 20 min, the cold wall temperature reaches 13.6 ºC, and it is kept in this value during the duration of the experiments. As expected, initially there was no deposit, therefore, the free flow area was the size of the radius gap ($gap = r_{ex} - r_{in}$) at the beginning. However, as the deposits is formed in inner radius, the free flow area varies.

Table 1. Parameters for simulation.

$L(m)$	$r_{int}(mm)$	$r_{ext}(mm)$	$\dot{\forall}_{in}(lt/min)$	$\rho_{in}(kg/m^3)$	$P_{out}\,(Pa)$	$T_{in}(°C)$	$T_{cold}(°C)$
1.05	9.5	17	3.5	750	101325	38	~14

To solve the present test case, a grid and time step test were performed, where variation of the deposit thickness was less than 2%. The mesh was defined with 75 control volumes in the axial direction and 60 for radial direction. The time-step chosen was equal to 0.1 s and after 10 min, it was increased to 1 s until the end of simulation.

3.1 Fluid

The mass concentration, which is the input data of thermodynamic model, is obtained through the molar concentration. The molar concentration of the mixture used is shown in Table 2, which is same as employed in the experimental setup. The WAT is between 34.5 °C and 35.5 °C.

Table 2. Carbon number and molar composition of mixture used.

carbon	molar concentration	carbon	molar concentration
12	0.9030000	31	0.007200
22	0.0000661	32	0.004630
23	0.0004590	33	0.002910
24	0.0024900	34	0.001810
25	0.0070000	35	0.001130
26	0.0121000	36	0.000720
27	0.0156000	37	0.000471
28	0.0160000	38	0.000316
29	0.0138000	39	0.000207
30	0.0105000		

4. RESULT

The Figure 1 shows a comparison of the numerical prediction with experimental data of the time evolution of the deposit thickness δ divided by the gap at the axial position at $z/L = 0.75$. Very good agreement is obtained for the first

10 min. After that, a very small increase of the wax deposition thickness is predicted, indicating that steady state regime was attained at approximately 25 minutes after the beginning of the process. At this position, the deposit thickness experimentally measured keeps increasing up to 30 min, reaching a larger value.

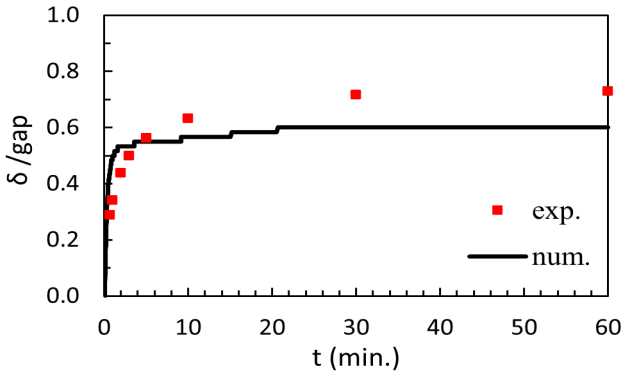

Figure 1. Comparison numerical versus experimental of time evolution of the deposit thickness at $z/L = 0.75$.

The spatial profile of the dimensionless deposit thickness, δ/gap, obtained with the present model is compared with the experimental measurements in Figure 2 for 5, 10 and 60 minutes. Note that the deposit thickness increases along the pipe and time due to the fluid cooling. The fluid close to the wall is cooled by the contact with the cold inner wall, and as time advances, the fluid in the core of the pipe is also cooled. When the temperature drops below WAT, solid particles are formed and when the solid volume fraction exceeds 2%, it is assumed that the deposit is formed, the velocity is set to zero, eliminating the flow convection.

Analyzing the results, one can observe that the numerical result, with the present simplified model, presents a similar profile as the measured data not only along the test section, but also as time increases. However, as already seen in the previous result, the numerical deposit thickness is sub-estimated, reaching steady state condition faster that was observed experimentally.

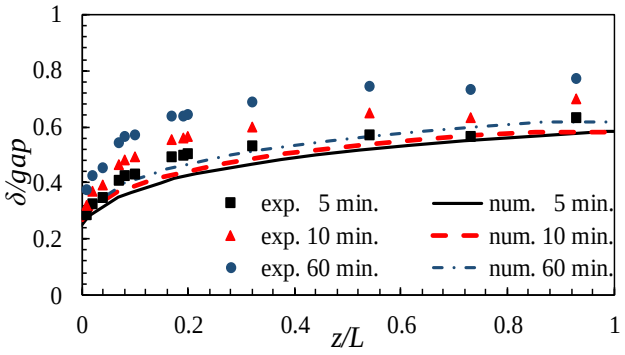

Figure 2. Comparison numerical versus experimental of axial variation of the deposit thickness at t =5, 10 and 60 min.

Figure 3 presents the radial temperature profiles obtained with the proposed model in two coordinates of the pipe, z / L = 0.25 and 0.75, after 5 and 60 minutes from the begging of the cooling. The change of the profile clearly indicates the deposit region, since inside the deposit, the temperature is the typical conduction profile (close to a straight line). Further, as already shown, the deposit thickness is larger far from the entrance, due to the lower fluid temperature. Note also, that, outside the deposit, convection is dominant, and the fluid temperature is almost equal to the inlet temperature. The temperature profiles are very similar for the two time instants, since a significant variation of the deposit thickness is only obtained in the first 5 min (Figure 1).

Figure 4 presents a comparison with the experimental data of the predicted temperature profile along the radial coordinate at $z/L = 0.75$ after 5 and 60 minutes of the beginning of the cooling process. Inside the figure, the dimensionless deposit thickness is indicated. The temperature is colder inside the deposit, it is governed by conduction and excellent agreement was obtained, especially for 60 min. Outside the deposit, convection is dominant and the temperature is almost uniform and close to the inlet value. Slightly cooler temperatures were predicted at the begging of the process inside the deposit, and practically identical temperatures outside. At t = 60 min, the experimental profile indicates a temperature reduction of the fluid side near the interface, perhaps due to axial diffusion, which was neglected in the numerical model. Note that the interface temperature is within the WAT interval indicated by the experimental measurements.

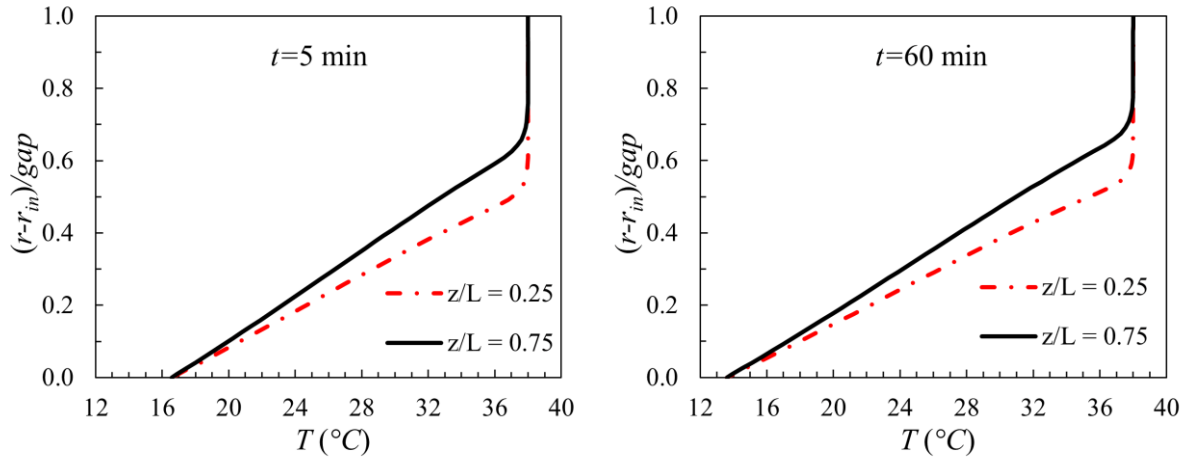

(a) 5 minutes (b) 60 minutes

Figure 3. Numerical radial temperature profile at $z / L = 0.25$ and 0.75, for time equal to 5 minutes and 60 minutes.

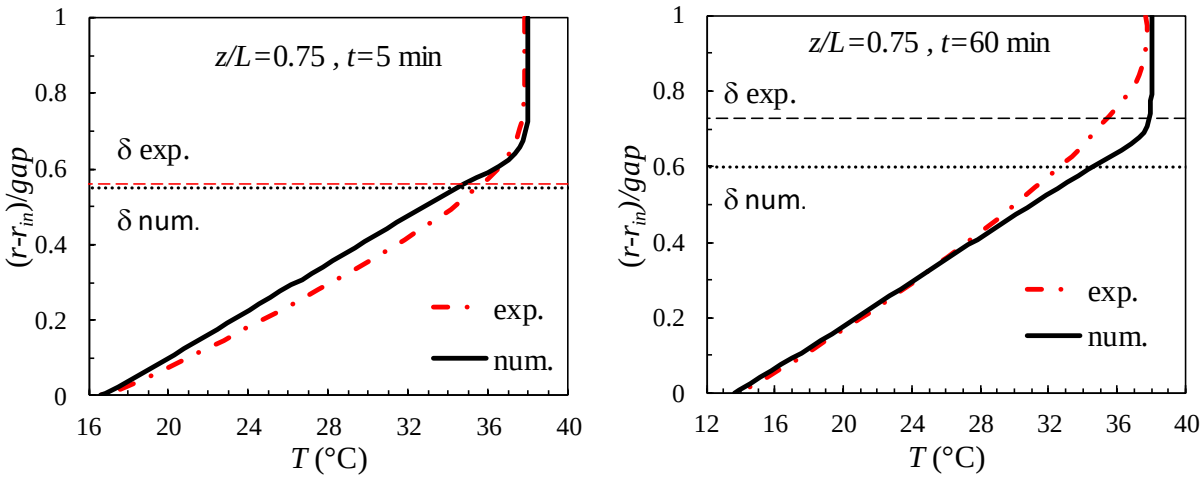

(a) 5 minutes (b) 60 minutes

Figure 4. Comparison of the experimental versus numerical radial temperature profile at $z / L = 0.75$, for time equal to 5 minutes and 60 minutes.

5. CONCLUSION

A simplified wax deposition model was proposed in the present work. The flow velocity and pressure are determined assuming the flow fully developed, and a 2D formulation is applied to determine the temperature. The model considers diffusion in the radial direction and convection in the axial direction, allowing to employ a 1D marching procedure. The fluid mixture properties are determined by interpolating data from a table constructed based on a multiple solid solutions thermodynamic model. The deposit is formed when solid volume fraction is above 2%. To validate the model, a comparison with laboratory data available in the literature was presented. The case studied was an annular duct flow in laminar regime. In comparison with experimental data, the model predicted reasonable results, but the deposit thickness was sub-estimated, although good agreement was obtained for the temperature profile.

6. ACKNOWLEDGEMENTS

The authors would like to thank to Coordenação de Aperfeiçoamento do Pessoal de Nível Superior – Brasil (CAPES) and to Conselho Nacional de Desenvolvimento Científico e Tecnológico – Brasil (CNPq) for their support to carry out this present work.

7. REFERENCES

Anisuzzaman, S. M., Abang, S., Bono, A., Krishnaiah, D., Karali, R., Safuan, M. K., 2017. “Wax inhibitor based on ethylene vinyl acetate with methyl methacrylate and diethanolamine for crude oil pipeline”. *IOP Conference Series: Materials Science and Engineering*, Vol. 206, No. 1, pp. 012074.

Azevedo, L. F. A., Teixeira, A. M., 2003. "A critical review of the modeling of wax deposition mechanisms". *Petroleum Science and Technology*, Vol. 21, No. 3-4, pp. 393-408.

Azevedo, L. F.A., Braga, A. M. B., Nieckele, A. O., Naccache, M. F., Gomes, M. G., 1996. "Simple hydrodynamic models for the prediction of pig motions in pipelines". In *Offshore Technology Conference*.

Branco, T.M.C.R., 2019. "Analysis of pigging gas pipelines in the presence of condensates" (in Portuguese). Master`s Dissertation, Graduate Program in Mechanical Engineering, Pontifical Catholic University of Rio de Janeiro, Rio de Janeiro, Brazil.

Burger, E., Perkins, T., Striegler, J., 1981. "Studies of Wax Deposition in the Trans Alaska pipeline". *Journal of Petroleum Technology*, Vol. 33, No. 06, pp. 1075-1086.

Coutinho, J. A., Mirante, F., Pauly, J., 2006. "A new predictive UNIQUAC for modeling of wax formation in hydrocarbon fluids". *Fluid phase equilibria*, Vol. 247, No. 1-2, pp. 8-17.

da Silva, V. M., do Carmo, R. P., Fleming, F. P., Daridon, J. L., Pauly, J., Tavares, F. W., 2017. "Paraffin solubility and calorimetric data calculation using Peng-Robinson EoS and modified UNIQUAC models". *Journal of Petroleum Science and Engineering*, Vol. 156, pp. 945-957.

Ehsani, S., Mehrotra, A. K., 2019. "Validating Heat-Transfer-Based Modeling Approach for Wax Deposition from Paraffinic Mixtures: An Analogy with Ice Deposition". *Energy & Fuels*, Vol. 33, No. 3, pp. 1859-1868.

Fleming, F. P, 2018, "Fundamental study of wax deposition under real flow conditions". Doctor Theses, Graduate Program in Mechanical Engineering, Pontifical Catholic University of Rio de Janeiro, Rio de Janeiro, Brazil.

Holder, G., Winkler, J., 1965. "Wax crystallization from distillate fuels: 1. cloud and pour phenomena exhibited by solutions of binary n-paraffin mixtures". *Journal of the Institute of Petroleum*, Vol. 51, No. 499, pp. 228-235.

Lira-Galeana, C., Firoozabadi, A., Prausnitz, J. M., 1996. "Thermodynamics of wax precipitation in petroleum mixtures". *AIChE Journal*, Vol. 42, No. 1, pp. 239-248.

Mahir, L. H. A., Vilas Bôas Fávero, C., Ketjuntiwa, T., Fogler, H. S., Larson, R. G., 2018. "Mechanism of Wax Deposition on Cold Surfaces: Gelation and Deposit Aging". *Energy Fuels*, Vol. 33, No. 5, pp. 3776−3786

Mehrotra, A. K., Ehsani, S., Haj-Shafiei, S., Kasumu, A. S., 2020. "A review of heat-transfer mechanism for solid deposition from "waxy" or paraffinic mixtures". *The Canadian Journal of Chemical Engineering*, Vol. 98, No. 12, pp. 2463-2488.

Palermo, T., Tournis, E., 2015. "Viscosity prediction of waxy oils: Suspension of fractal aggregates (SoFA) model". *Industrial & Engineering Chemistry Research*, Vol. 54, No. 16, pp. 4526-4534.

Queimada, A. J., Marrucho, I. M., Coutinho, J. A. P., Stenby, E. H., 2005. "Viscosity and liquid density of asymmetric n-Alkane mixtures: Measurement and modeling". *International Journal of Thermophysics*, Vol. 26, No. 1, pp. 47–61.

Singh, P., Fogler, H. S., Nagarajan, N., 1999. "Prediction of the wax content of the incipient wax-oil gel in a pipeline: An application of the controlled-stress rheometer". *Journal of Rheology*, Vol. 43, No. 6, pp. 1437-1459.

Singh, P., Venkatesan, R., Fogler, H. S., Nagarajan, N., 2000. "Formation and aging of incipient thin film wax-oil gels". *AIChE journal*, Vol. 46, No. 5, pp. 1059-1074.

Todi, S., Deo, M., 2006. "Experimental and modeling studies of wax deposition in crude-oil-carrying pipelines". *Offshore technology conference*.

Van Der Geest, C., Guersoni, V. C. B., Merino-Garcia, D., Bannwart, A. C., 2018. "Wax deposition experiment with highly paraffinic crude oil in laminar single-phase flow unpredictable by molecular diffusion mechanism". *Energy & Fuels*, Vol. 32, No. 3, pp. 3406-3419.

Veiga, H. M., Boher e Souza, L., Fleming, F. P., Ibanez, I., Linhares, R. C., Nieckele, A. O., Azevedo, L. F. A., 2020. "Experimental and Numerical Study of Wax Deposition in a Laboratory-Scale Pipe Section under Well-Controlled Conditions". *Energy & Fuels*, Vol. 34, No. 10, pp. 12182-12203.

Zheng, S., Saidoun, M., Mateen, K., Palermo, T., Ren, Y., Fogler, H. S., 2016. "Wax deposition modeling with considerations of non-newtonian fluid characteristics". *Offshore Technology Conference*.

8. RESPONSIBILITY NOTICE

The authors are the only responsible for the printed material included in this paper.